Intensive Care Med (1998) 24: 1209–1216
© Springer-Verlag 1998

EXPERIMENTAL

R.P. Stidwill
D.M. Rosser
M. Singer

Cardiorespiratory, tissue oxygen and hepatic NADH responses to graded hypoxia

Received: 2 April 1998
Accepted: 26 August 1998

This work was supported by a grant from the Sir Jules Thorn Charitable Trust

R.P. Stidwill · D.M. Rosser · M. Singer (✉)
Bloomsbury Institute of Intensive Care Medicine, Department of Medicine, University College London Medical School, Rayne Institute, University Street, London WC1E 6JJ, UK
e-mail: m.singer@ucl.ac.uk
Tel. + 44(171)209–6208;
Fax + 44(171)209–6258

Abstract *Objective*: To assess cardiorespiratory, tissue oxygen and hepatic nicotine adenine dinucleotide hydride (NADH) responses to graded hypoxia.
Design: Prospective, controlled, randomized study.
Setting: University laboratory.
Animals and interventions: 18 anaesthetised Sprague-Dawley rats spontaneously breathing either 21 % (controls), 12.5 % or 10 % inspired oxygen concentrations (6 rats per group).
Measurements and results: All animals in the 21 and 12.5 % O_2 groups survived the 3-h study period, compared to only 1 in the 10 % O_2 group. In this latter group, mean arterial pressure and renal blood flow fell immediately with hypoxaemia, whereas aortic blood flow was maintained until the preterminal stages. Critical cellular hypoxia was suggested by an increasingly severe base deficit, an initial rise then a preterminal fall in hepatic NADH intensity and premature death in all but 1 animal. Hepatic NADH fluorescence intensity was unchanged in control animals but showed a progressive rise in the 12.5 % O_2 group, accompanied by a small though static increase in arterial base deficit. No significant differences were seen in arterial and tissue partial pressure of oxygen between the 12.5 and 10 % O_2 groups.
Conclusions: This study demonstrates major differences in cardiorespiratory, hepatic NADH and outcome responses to small variations in the degree of hypoxic hypoxia. The fall in NADH fluorescence intensity presages impending death and is likely to reflect failure of cellular metabolic processes.

Key words Tissue oxygen · NADH · Hypoxic hypoxia · Hypoxaemia · Haemodynamics

Introduction

Cellular hypoxia is the ultimate defect in many clinical conditions leading to organ failure and death – for example, haemorrhage, hypoxaemia and cardiac failure. The development of cellular hypoxia is dependent on many factors including haemoglobin concentration, cardiac output, microvascular integrity, arterial oxygenation and cellular oxygen demands. In both the laboratory and, in particular, the clinical situation, several of these factors are liable to change concurrently.

Nicotine adenine dinucleotide hydride (NADH) concentrations reflect the redox potential at complex I of the mitochondrial respiratory chain. In the absence of any respiratory chain poison this will reflect the availability of oxygen at complex IV, the only oxygen-consuming reaction in oxidative phosphorylation. A simplified schema is shown in Fig. 1. Changes in hepatic mitochondrial NADH concentration are reflected by changes in NADH surface fluorescence intensity [1–4]. Sequential changes of this variable in a lethal model of hypoxic hypoxia have not been previously examined.

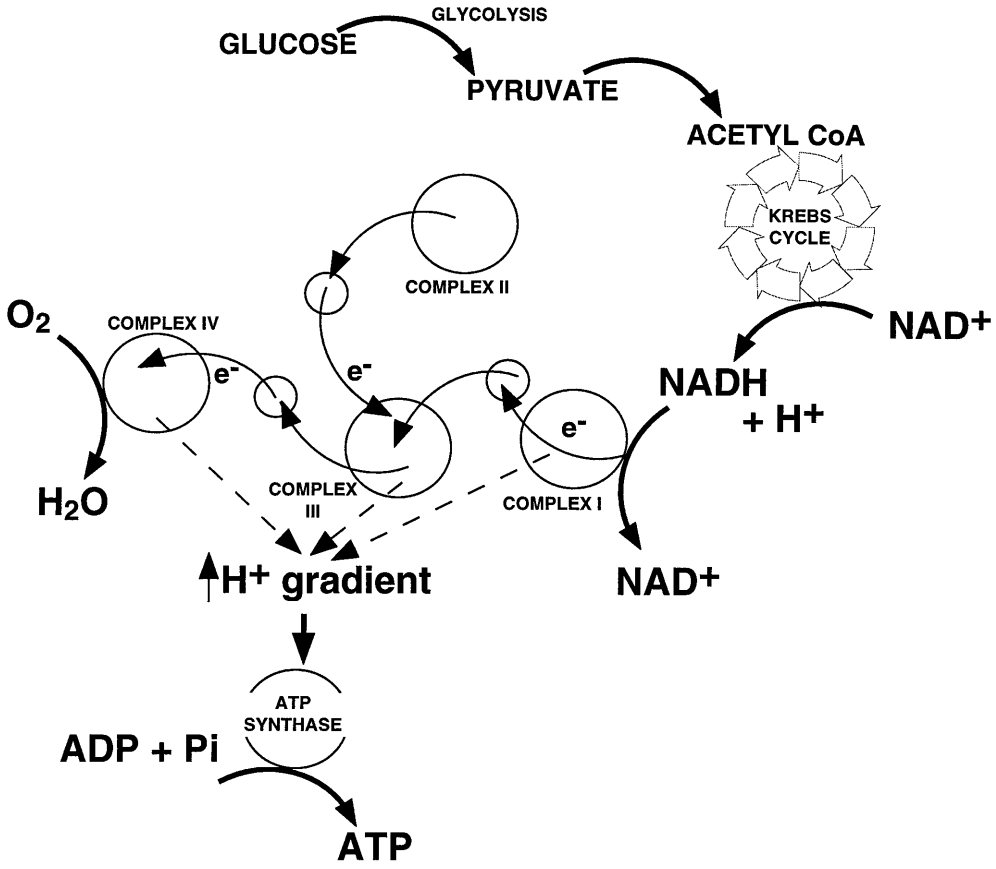

Fig. 1 Schematic representation of the electron transport chain. Electron e^- transfer, shown by *arrowed route* through to complex IV, creates a H^+ gradient across the inner mitochondrial gradient which is sufficient to drive generation of ATP by ATP synthase

This technique was thus utilised in an anaesthetised, spontaneously breathing rat model of hypoxic hypoxia to examine the relationship between changes in NADH surface fluorescence intensity, concurrently measured markers of tissue oxygenation and cardiorespiratory status and progression to death.

Materials and methods

Anaesthesia and surgery

These experiments were performed under United Kingdom Home Office approval according to the Animals (Scientific Procedures) Act 1986. Male Sprague-Dawley rats of 250–300 g body weight were given free access to food and water until the time of surgery. Anaesthesia was induced by placing the rats in a glass tank and introducing 5% isoflurane in air by a pump driving a Tec 4 vaporiser (Abbott, Maidenhead, UK). Once anaesthesia was established, the animal was placed on a heated operating table to maintain the rectal temperature between 37 and 38 °C. During instrumentation, anaesthesia was maintained with 1–2% isoflurane via a face mask, adjusted according to the degree of surgical stimulation. Thereafter, isoflurane was administered at a dose of 1.2% continuously throughout the experimental period.

The model preparation (except for the NADH surface fluoroscopy) is described in detail elsewhere [5–7]. Briefly, the right internal jugular vein is cannulated and connected to an infusion pump through which an intravenous bolus of 4 ml/kg 0.9% saline followed by an infusion of 20 ml/kg per h is given. The left carotid artery is then cannulated for continuous monitoring of blood pressure (pressure transducer MX860, Medex, Haslington, UK) and monitor 78353A (Hewlett Packard, Bracknell, UK) and intermittent sampling for arterial blood gas analysis (165 µl heparinized capillary tube samples, processed by an ABL4 analyser, Radiometer, Copenhagen, Denmark). The trachea is cannulated and a T-piece fitted to this tracheotomy tube and adjusted to approximate anatomical dead space; anaesthesia is then continued via this route.

A midline laparotomy is performed. Doppler ultrasound flow probes are placed on the left renal artery (1 mm, J-reflector-1RB) and infra-renal abdominal aorta (2 mm, J reflector-2SB) and connected to a flow monitor (Model T206, Transonic Systems, Ithaca, N. Y., USA). The bladder is exposed and a small incision made in its avascular dome through which is passed a drainage cannula (1.57 mm outside diameter) and a previously calibrated polarographic oxygen electrode of active length 10 mm and diameter 0.55 mm (Continucath, Biomedical Sensors, High Wycombe, UK). The electrode is inserted until a 15-mm length is seen to indent the bladder wall, thus ensuring good contact between active electrode and bladder epithelium. The electrode and drainage cannula are then secured by a ligature around the wound. Finally, a thermistor is inserted into the rectum.

For NADH measurements, a luminescence spectrometer (Model LS-50B, Perkin Elmer, Beaconsfield, Bucks., UK) was used. A fibreoptic cable from the machine was sheathed in a clear,

rigid plastic tube protruding 5 mm from the end of the cable fixed. The cable was lowered by a manipulating arm until the end of the plastic sheath was just touching the surface of the left lobe of the liver throughout respiration. The cable was thus held still, but not compressed, at a set distance from the liver surface. Scanning was performed using 340-nm excitation light and recording emissions between 360 and 640 nm using an excitation slit width of 5 nm and an emission slit of 20 nm. NADH fluorescence intensity was taken as the height of the peak at 460 nm. Subsequent correction for interference was not found to be necessary as interference was excluded beforehand by two different control experiments. Firstly, sham-operated control animals were subjected to isovolaemic haemodilution to change the total concentration of haemoglobin. Secondly, another group of animals was exposed to 15% inspired oxygen to increase deoxyhaemoglobin concentration without causing cellular hypoxia. In neither group was there a significant change in NADH fluorescence intensity or metabolic acidosis (unpublished data). Thus NADH data presented here are not mathematically manipulated. Successive recordings were made over 2 min and the average of three measures falling within 5% of each other taken. In practice, a fourth scan was rarely necessary. To reduce the risk of bleaching, excitation was performed over 6–8 min at 15-min intervals. No obvious bleaching was seen macroscopically.

Experimental protocol

The animals were left to stabilise for 30 min after surgery. Baseline recordings of all measured variables were taken and repeated after a further 15 min to ensure stability. After the second set of baseline readings, two groups of six animals were changed from room air to either 12.5% O_2 in nitrogen (12.5% O_2 group) or 10% O_2 in nitrogen (10% O_2 group). The third group of six animals was maintained on room air to act as sham operated controls (21% O_2 group). The hypoxic mixtures were delivered from a gas blender blending pure O_2 and N_2, via the isoflurane vaporiser, keeping the concentration of isoflurane unchanged. The O_2 content of the gas mix was verified at intervals by passing samples through the blood gas analyser. Measured variables were recorded every 15 min.

Data analysis

Flow data were converted to ml/min per kg body weight. Bladder oxygen tension data were temperature corrected retrospectively using the recommended correction factor of 4% per degree Celsius. Blood gas data were temperature corrected at analysis by the blood gas machine. As NADH fluorescence intensity is recorded on an arbitrary scale, this variable was analysed by examining percentage change from baseline. Analysis of variance with post hoc Fisher's test was used to determine any statistically significant changes.

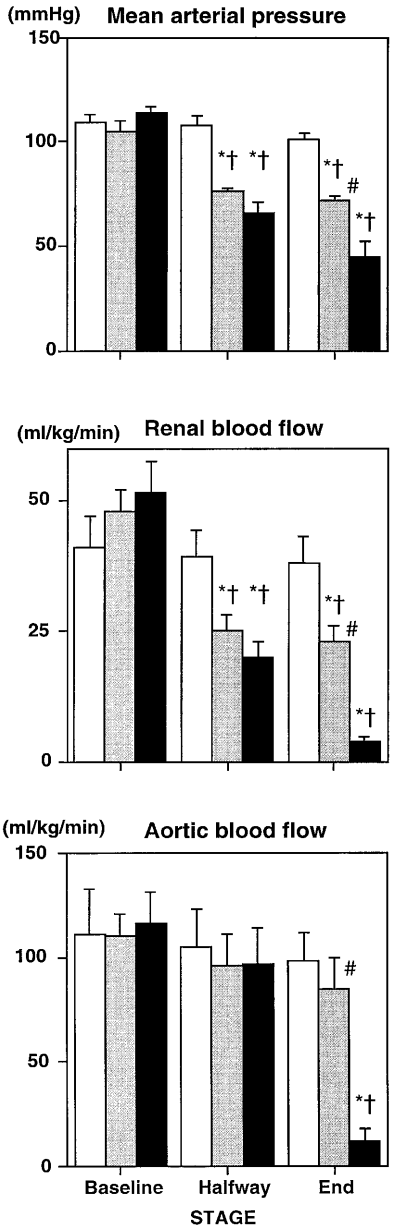

Fig. 2 Changes (mean ± SEM) in mean arterial blood pressure *top panel*, renal blood flow *middle panel* and aortic blood flow *bottom panel* at baseline, midstage of the experiment and endstage (either 3 h or preterminal). The 21% O_2 (control) group is represented by *white columns*, the 12.5% group by *grey columns* and the 10% group by *black columns*. Statistical significance ($p < 0.05$) shown by * for group versus control, † for group versus baseline and # for the 10% group versus the 12.5% group

Results

All six animals in the 21 and 12.5% O_2 groups survived the 3-h study period. Only one of the six animals in the 10% O_2 group survived, the others dying between 60 and 105 min (median survival time 84 min). Due to the differing lengths of the experiments, the data are presented for clarity as baseline, midstage (halfway through the experiment) and endstage (the last reading taken before the animals died or at 180 min) values. No changes were seen between the two baseline values in any variable, therefore the second set of baseline data was used throughout.

No significant differences were seen in body weight or baseline physiological values between any of the

three groups. There were no significant changes in the sham-operated group for any measured variable over the 3-h period. Temperature did not change significantly in any group and no differences were seen between groups. No bladder O_2 electrode was found to have drifted by more than 2% at the end of the study.

Mean arterial pressure (MAP) fell rapidly in the 12.5 and 10% groups on introduction of hypoxaemia. Significant differences were found at mid- and endstages, with the fall in MAP in the 10% O_2 group being greater than in the 12.5% O_2 group. The same pattern was seen for renal blood flow, whereas aortic blood flow was unchanged until the endstage in the 10% O_2 group (Fig. 2).

Bladder epithelial oxygen tension and arterial oxygen tension (PaO_2) fell significantly in both hypoxaemic groups (Fig. 3). Although values were initially lower in the 10% O_2 group, no significant difference in oxygen tensions were seen between the two hypoxaemic groups at either mid- or endstages. PaO_2 rose significantly in the 10% group between mid- and endstages in line with the increasing metabolic acidosis.

Arterial pH rose significantly by midstage and remained elevated at endstage in the 12.5% O_2-group; in the 10% O_2 group arterial pH did not change by midstage but fell significantly at endstage. The arterial base deficit was significantly greater at midstage in the 12.5% O_2 group compared to sham-operated animals but thereafter remained constant. In the 10% O_2 group the arterial base deficit was significantly greater than the 12.5% O_2 group by midstage and increased still further by endstage. Arterial carbon dioxide tension ($PaCO_2$) fell significantly in both hypoxic groups at midstage compared to both sham-operated animals and to baseline values; thereafter it remained unchanged (Fig. 4).

Hepatic NADH fluorescence intensity initially rose significantly in the 10% O_2 group before falling below baseline as a preterminal phenomenon. Figure 3 shows pooled group data for percentage change in NADH intensity, while Fig. 5 displays the data from individual animals measured at 15-min intervals.

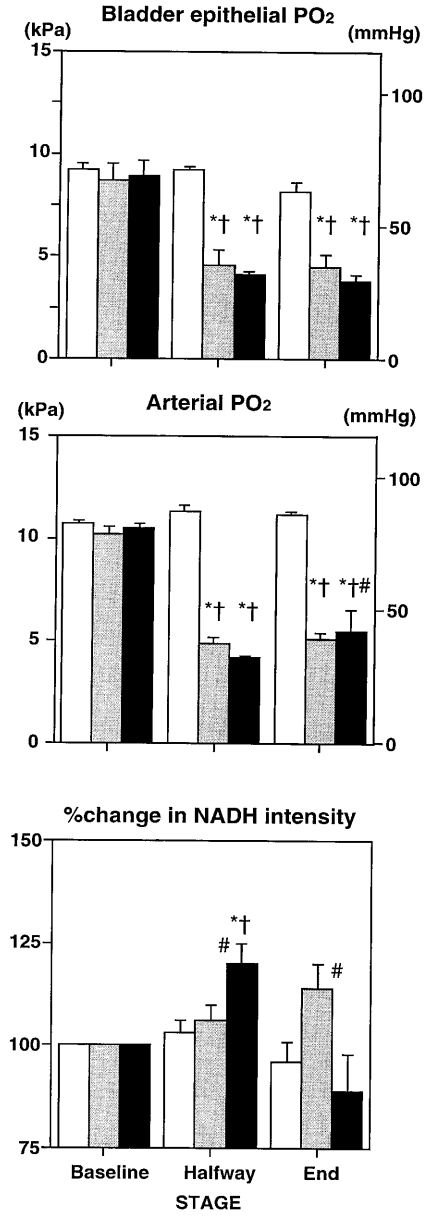

Fig. 3 Changes (mean ± SEM) in bladder epithelial oxygen tension *top panel*, arterial oxygen tension *middle panel* and percentage change in hepatic surface NADH fluorescence intensity *bottom panel* at baseline, midstage of the experiment and endstage (either 3 h or preterminal). The 21% O_2 (control) group is represented by *white columns*, the 12.5% group by *grey columns* and the 10% group by *black columns*. Statistical significance ($p < 0.05$) shown by * for group versus control, † for group versus baseline and # for the 10% group versus the 12.5% group

Discussion

We have previously used a similar rat model to assess changes in tissue oxygenation following various physiological insults including haemorrhage, drugs and endotoxaemic sepsis [5–7]. This present study investigating hypoxic hypoxia revealed a similar pattern to progressive haemorrhage in terms of blood flow and pressure, an increasing metabolic acidosis, compensatory hyperventilation and falls in tissue oxygen tension measured at the bladder epithelium [5].

To our knowledge, this is the first in vivo study of hepatic NADH during hypoxic hypoxia with measurements made sequentially until death. NADH is the major contributor of high energy electrons to the respiratory chain and is converted to NAD^+ in the process. NADH but not NAD^+ fluoresces in response to excitation light at 340 nm and is the only biological compound

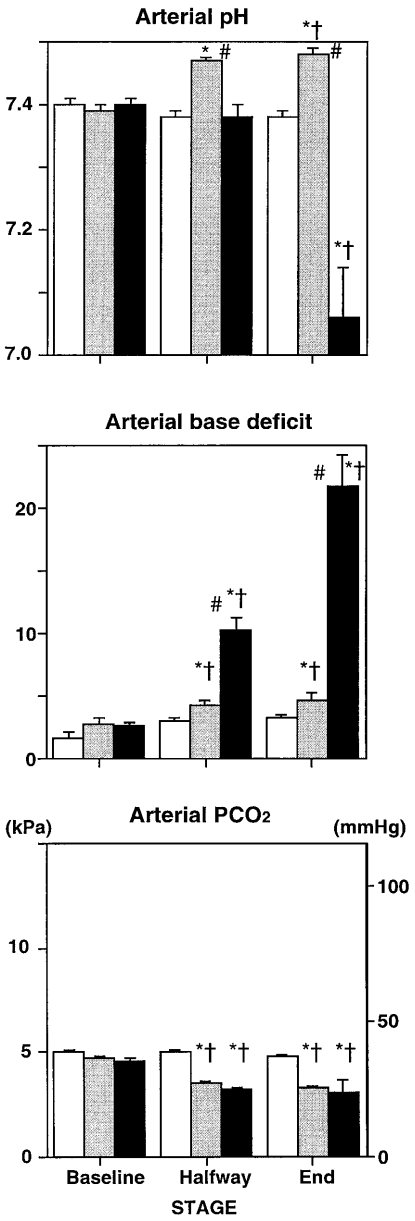

Fig. 4 Changes (mean ± SEM) in arterial pH *top panel*, arterial base deficit *middle panel* and arterial PCO_2 *bottom panel* at baseline, midstage of the experiment, and endstage (either 3 h or preterminal). The 21 % O_2 (control) group is represented by *white columns*, the 12.5 % group by *grey columns* and the 10 % group by *black columns*. Statistical significance ($p < 0.05$) shown by * for group versus control, † for group versus baseline and # for the 10 % group versus the 12.5 % group

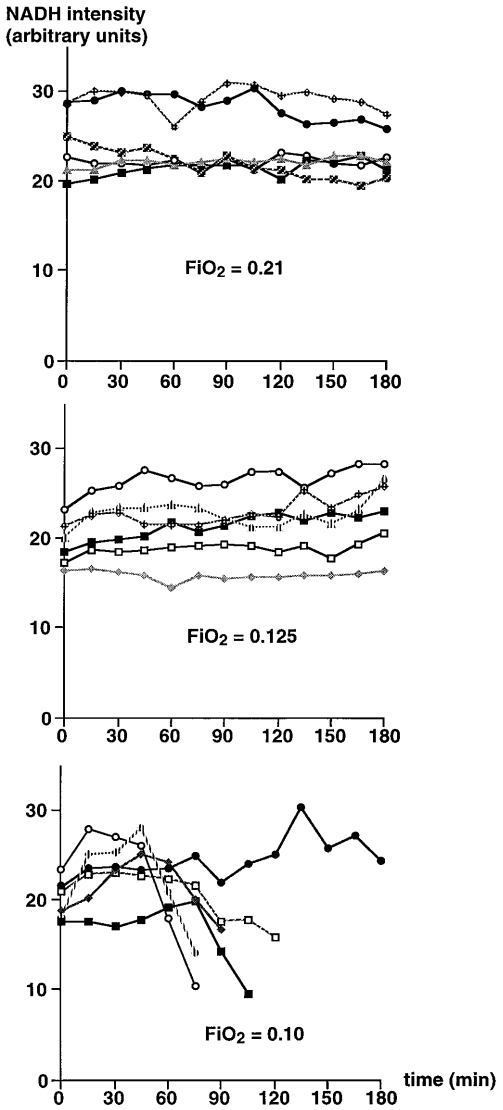

Fig. 5 Changes in hepatic surface NADH fluorescence intensity for individual animals taken at 15-min intervals

to do so [1]. The light intensity emitted by this fluorescence is related to the intensity of the excitation light and the concentration of the fluorescent compound. NADH fluorescence is quenched by a number of cytosol constituents which are not found within the mitochondrion, thus most of the signal seen represents changes in mitochondrial NADH [2–4]. In the absence of changes in the total NADH/NAD^+ pool, a rise in [NADH] reflects decreased oxygen availability to the mitochondrial respiratory chain. This has previously been observed in brains rendered ischaemic [8]. The subsequent and preterminal fall in NADH to below baseline suggests that production of NADH may have become impaired, consistent with a failure of cellular metabolic processes. Identical findings of an initial rise then irreversible decline in NADH fluorescence were made in rat hepatocyte suspensions and isolated perfused liver rendered hypoxic [9]. The decline in NADH fluorescence correlated with decreased cell viability. With brief periods of hypoxia, ATP concentrations fell but recovered upon reoxygenation; however, with longer peri-

ods of hypoxia, the fall in [ATP] was more profound with incomplete recovery on reoxygenation. In vivo, this mitochondrial NADH oxidation may be brought about by inadequacy of substrate supply [10], mimicking state II mitochondrial respiration where substrate rather than oxygen supply is limiting. The degree of mitochondrial NADH oxidation at which cellular damage and energy depletion become irreversible remains to be elucidated.

NADH fluoroscopy is a well established technique [1]. There are a number of recognised potential sources of measurement error, e.g., changes in ambient light, distance between probe and tissue, direct tissue pressure by the probe, and reflectance and absorbance of emission light. Changes in ambient light were easily excluded by performing the scans in the dark. Changes in reflectance and probe to liver distance were minimised by using the sheath around the end of the fibreoptic probe which held the liver at the same angle and distance from the probe for each measurement. The probe was lifted from the liver between each scan to prevent any interference from continuing local pressure ischaemia and to reduce the risk of bleaching. By holding the probe in a manipulator so that it touched yet did not exert any significant pressure on the liver surface, it is unlikely that surface blood flow would be compromised thereby introducing measurement artefacts. The main compound with the potential to cause absorption artefacts is haemoglobin, particularly deoxyhaemoglobin. A number of corrections take this into account [3]; however, application of these to our data made no difference to either trends or statistical significance. Variability of three successive measurements performed within 2 min was approximately 3%, though this did increase in the immediate premortem period.

Haemodynamic responses were essentially similar in both hypoxaemic groups until those animals exposed to 10% oxygen reached a preterminal state. The one survivor in the 10% O_2 group paralleled the 12.5% O_2 group response. Measurements of arterial base deficit and hepatic NADH fluorescence intensity, however, revealed significant increases which occurred much earlier in the 10% O_2 group despite concurrently measured cardiorespiratory variables being comparable to the 12.5% O_2 group. The rise in NADH fluorescence intensity and the severe metabolic acidosis in the 10% group thus suggest severe tissue hypoxia, which was evidenced in this study by premature death in five of the six animals. The 12.5% O_2 group also developed an increasing arterial base deficit by the midstage, though this did not progress further. Until the terminal stages, this metabolic acidosis was well compensated for by a hyperventilation-generated respiratory alkalosis.

The rapid reduction in renal blood flow – in contrast to aortic flow – seen in both groups after induction of hypoxaemia was similar in timing and magnitude to the fall in MAP. This relationship, which we have also documented with haemorrhage, sepsis and vasoactive drugs [5–7], suggests that renal perfusion in the rat is pressure-dependent. However, $PaCO_2$ changes are also known to have a significant effect on renal blood flow in the hypoxic rat [11, 12], and this may also contribute to the changes seen in this spontaneously breathing model. An alternative approach would be to ventilate the animals mechanically and maintain normocapnia. However, we chose not to utilise this approach as it would prevent the normal physiological response to hypoxaemia and would require a higher level of anaesthesia that would likely affect haemodynamic responses and regional blood flows to a much greater degree. Rats anaesthetised with volatile anaesthetics (halothane, enflurane or isoflurane) and rendered hypoxaemic [fractional inspired oxygen ((FIO_2) 0.12 for 20 min] showed significant decreases in renal, gastrointestinal and hepatic blood flows compared to awake, non-anaesthetised animals [13]. The abstract from a Japanese paper [14] suggested that isoflurane was superior to sevoflurane and halothane in maintaining hepatic circulation in severely hypoxaemic rats (FIO_2 0.08).

Ideally, we would like to have assessed temporal changes in NADH, blood flow and tissue oxygen tension in the same organ following an insult. However, our rat model precludes instrumentation of the hepatic vein, or the portal vein plus hepatic artery, to enable continuous monitoring of total hepatic blood flow, and we sought to avoid invasive monitoring of hepatic parenchymal PO_2. Studies of regional blood flow during hypoxaemia have revealed flow redistribution with maintenance of flow to the coronary and cerebral beds at the expense of renal, splanchnic and pancreatic circulations [13, 15, 16]. Total hepatic blood flow is maintained during mild or moderate hypoxaemia but falls significantly with severe hypoxaemia (FIO_2 0.10) [14, 17]. Measurement of tissue PO_2 at the bladder epithelium does, however, appear to be a sensitive indicator of the balance between oxygen supply and demand and reflects findings measured during cardiorespiratory insults at other sites including muscle and liver [18, 19]. Though in this present study the bladder epithelial PO_2 predictably fell with progressive lowering of the inspired oxygen concentration, other cardiovascular insults have shown a dissociation between arterial and bladder tissue PO_2 [5–7]. Indeed, the bladder epithelial PO_2 failed to rise at endstage in the 10% FIO_2 group despite the significant increase seen in arterial PO_2 due to attempted respiratory compensation. The bladder epithelium could prove to be a readily accessible and useful surrogate of tissue PO_2 in other, more vital, organs though this requires validation. However, the approximate 5 mmHg (0.67 kPa) difference in bladder epithelial PO_2 values between the two hypoxaemic groups, albeit statistically significant, is probably unable to differentiate

in clinical terms between critical and non-critical hypoxic hypoxia.

No statistical or clinically significant differences occurred in arterial PO_2 between the two hypoxic groups at any point. The PaO_2 level cannot therefore be used to indicate the point at which hypoxic hypoxia becomes critical. The significant endstage rise in PaO_2 in the 10 % O_2 group was coincident with the increasing metabolic acidosis and has been previously documented with other insults studied in this spontaneously breathing model [5–7]. It is not fully accounted for by the alveolar gas equation and the compensatory hyperventilation-induced fall in $PaCO_2$. Furthermore, the combination of an acidosis-induced right shift in the oxyhaemoglobin dissociation curve plus the severe preterminal fall in aortic blood flow with increased tissue oxygen extraction would promote a fall rather a rise in arterial oxygen tension. We are thus unable to explain this finding.

The respiratory chain appears capable of acting as an oxygen sensor through the physiological range [20–22]. Furthermore, cellular respiration and oxygen consumption are slowed by incubation at low physiological PO_2 [9, 22]. As tissue PO_2 represents the balance between oxygen supply and demand [23], a reduction in cellular respiration would explain the decreased difference between arterial and tissue PO_2 in the hypoxic animals. This mechanism would be protective and could explain the tolerance to relatively severe hypoxia shown by the animals in the 12.5 % O_2 group. Exceeding the limits of this protection may also explain how such severe metabolic derangements could be consequent to a small further reduction in oxygen tension.

In conclusion, the fall in tissue PO_2 seen in this model of hypoxaemia results in cellular hypoxia as evidenced by an increasing arterial base deficit and a rise in hepatic surface NADH fluorescence intensity. The demise of the animal is, however, preceded by a precipitate fall in surface NADH intensity values. The difference in oxygen tension between rapidly fatal hypoxic hypoxia and that which is survivable, at least in the short term, is relatively small. In this context, the monitoring of arterial PO_2 is unlikely to be helpful in identifying the point at which critical hypoxia ensues. Further study is needed to assess the utility of tissue PO_2 measurement and the possibility of using surrogate yet easily accessible regional beds such as the bladder epithelium as a means of monitoring critical tissue PO_2 in vital organs. Identifying the onset of metabolic acidosis is helpful in this simple model of hypoxic hypoxia but may be less useful in the more complex clinical situation. This model utilising concurrent measurement of oxygen tensions, haemodynamic variables and NADH fluoroscopy has considerable potential for the investigation of many of the conditions leading to critical illness. It also emphasises the need for further work to develop bedside measurement techniques which can monitor cellular hypoxia directly rather than indirectly.

Acknowledgements We gratefully acknowledge the assistance given by Dr. Maureen Thorniley

References

1. Chance B, Graham N, Mayer D (1971) A time sharing fluorometer for the readout of intracellular oxidation-reduction states of NADH and flavoprotein. Rev Sci Instrum 42: 951–957
2. Ince C, Ashruf JF, Sanderse EA, Pierik EG, Coremans JM, Bruining HA (1992) In vivo NADH and Pd-porphyrin video fluori-/phosphorimetry. Adv Exp Med Biol 317: 267–275
3. Ince C, Coremans JM, Bruining HA (1992) In vivo NADH fluorescence. Adv Exp Med Biol 317: 277–296
4. Thorniley MS, Simpkin S, Fuller B, Jenabzadeh MZ, Green CJ (1995) Monitoring of surface mitochondrial NADH levels as an indication of ischemia during liver isograft transplantation. Hepatology 21: 1602–1609
5. Singer M, Millar C, Stidwill RP, Unwin R (1995) Bladder epithelial oxygen tension – a new means of monitoring regional perfusion? Preliminary study in a model of exsanguination/fluid repletion. Intensive Care Med 22: 324–328
6. Rosser DM, Stidwill R P, Millar CG, Singer M (1995) The effect of norepinephrine and dobutamine on bladder epithelial oxygen tension. Chest 108: 1368–1372
7. Rosser DM, Stidwill RP, Jacobson DJ, Singer M (1996) Cardio-respiratory and tissue dose response to rat endotoxemia. Am J Physiol 271:H891–H895
8. Duckrow RB, LaManna JS, Rosenthal M (1981) Disparate recovery of resting and stimulated oxidative metabolism following transient ischemia. Stroke 12: 677–686
9. Obi-Tabot TE, Hanrahan LM, Cachecho R, Beer ER, Hopkins SR, Chan JC, Shapiro JM, LaMorte WW (1993) Changes in hepatocyte NADH fluorescence during prolonged hypoxia. J Surg Res 55: 575–580
10. Yager JY, Brucklacher RM, Vannucci RC (1991) Cerebral oxidative metabolism and redox state during hypoxia-ischemia and early recovery in immature rats. Am J Physiol 261: H1102–H1108
11. Walker BR, Brizzee BL (1988) Renal vascular response to combined hypoxia and hypercapnia in conscious rats. Am J Physiol 254: R552–R558
12. Zillig B, Schuler G, Truniger B (1978) Renal function and intrarenal hemodynamics in acutely hypoxic and hypercapnic rats. Kidney Int 14: 58–67
13. Durieux ME, Sperry RJ, Longnecker DE (1992) Effects of hypoxemia in regional blood flows during anesthesia with halothane, enflurane or isoflurane. Anesthesiology 76: 402–408
14. Sugai M (1996) Comparison of the effect of isoflurane and that of sevoflurane on hepatic circulation and oxygen metabolism during acute hypoxia in dogs. Masui 45: 608–616
15. Hoka S, Bosnjak ZJ, Arimura H, Kampine JP (1989) Regional venous outflow, blood volume and sympathetic nerve activity during severe hypoxia. Am J Physiol 256: H162–H170

16. Krasney JA, Hajduczok G, Miki K, Matalon S (1985) Peripheral circulatory responses to 96 hours of eucapnic hypoxia in conscious sheep. Respir Physiol 59: 197–211
17. Larsen JA, Krarup N, Munck A (1976) Liver hemodynamics and liver function in cats during graded hypoxic hypoxemia. Acta Physiol Scand 98: 257–262
18. Boekstegers P, Weidenhofer S, Pilz G, Werdan K (1991) Peripheral oxygen availability within skeletal muscle in sepsis and septic shock: comparison to limited infection and cardiogenic shock. Infection 19: 317–323
19. Nordin A, Makisalo H, Hockerstedt K (1994) Dopamine infusion during resuscitation of experimental hemorrhagic shock. Crit Care Med 22: 151–156
20. Nuutinen EM, Wilson DF, Erecinska M (1984) Mitochondrial oxidative phosphorylation: tissue oxygen sensor for regulation of coronary flow. Adv Exp Med Biol 169: 351–357
21. Wilson DF, Mokashi A, Chugh D, Vinogradov S, Osanai S, Lahiri S (1994) The primary oxygen sensor of the cat carotid body is cytochrome a3 of the mitochondrial respiratory chain. FEBS Lett 351: 370–374
22. Duranteau J, Chandel NS, Kulisz A, Shao Z, Schumacker PT (1998) Intracellular signalling by reactive oxygen species during hypoxia in cardiomyocytes. J Biol Chem 273: 11619–11624
23. Harper SL, Pitts VH, Granger DN, Kvietys PR (1986) Pancreatic tissue oxygenation during secretory stimulation. Am J Physiol 250: G316–G322